Biochemistry

 Volume 37, Number 7 February 17, 1998

New Concepts in Biochemistry

Amyloid Fibrils May Be Assembled from β-Helical Protofibrils†

N. D. Lazo and Donald T. Downing*

The Marshall Research Laboratories, Department of Dermatology, University of Iowa College of Medicine, Iowa City, Iowa 52242

Received April 30, 1997; Revised Manuscript Received October 21, 1997

Spectroscopic and X-ray crystallographic studies have rigorously defined the β-helical conformations of several proteins, including pectate lyases C (PelC) and E (PelE) (*1*−*4*), a phage tailspike protein (TSP) (*5*), and an acyltransferase (LpxA) (*6*), in each of which a single chain of short β-strands is wound into successive turns of parallel β-helix. In this study, further insight into the β-helical conformation was obtained by the construction of graphical and space-filling models of the established pectate lyase conformations. From these constructions, it appeared that the β-sheet conformations that have been proposed for the amyloid fibrils that are associated with a number of human diseases may actually be coiled into β-helixes. This speculation is illustrated herein by novel graphical expressions of pectate lyase conformations that were established previously by X-ray diffraction (*3*). By analogy, sequences found in three amyloid proteins—the Alzheimer Aβ protein, an immunoglobulin light-chain derivative (Rei), and transthyretin (TTR)—were modeled in plausible β-helical conformations. We propose these conformations as the basis for the 2−3 nm diameter protofibrils that recently have been recognized as subunits of the 7−13 nm diameter TTR and Aβ amyloid fibrils (*7*, *8*). Our postulated antiparallel arrangement of the amyloid protein chains in β-helixes complies with published spectroscopic and X-ray crystallographic properties of amyloid fibrils (*9*).

† Supported in part by NIH Grant AR32374 and by a bequest from the Carl J. Hertzog Foundation.

* Corresponding author at 270 Medical Laboratories, University of Iowa College of Medicine, Iowa City, IA 52242. Telephone: (319) 335-8080. Fax: (319) 335-9559. E-mail: nlazo@blue.weeg.uiowa.edu.

Pectate Lyase Conformations

X-ray crystallographic studies of pectate lyases have spelled out the spatial relationships between the amino acid residues shown to occupy positions in β-helixes (*1*). Figure 1 shows our representation of the β-helical regions of PelC and PelE, showing the predominantly hydrophobic nature of the amino acid side chains that are assigned to the helix lumen. The previous investigators proposed that the β-helical conformations are stabilized by hydrogen bonding between successive turns of the peptide backbone, between residues on the exterior of the helix, and between residues in loops of random coil projecting from successive turns of the central helix (*1*−*3*, *5*, *6*). Yoder et al. (*1*−*3*) also noted the ladders of external asparagine residues in PelC, and asparagine/serine residues in PelE (shown in red in Figure 1), that would contribute to the side chain hydrogen bonding for most of the length of each β-helix. By analogy with the pectate lyases, we have been able to construct β-helical conformations of amyloid protofibrils, based on published experimental data on these unsolved structures.

Amyloid Proteins

More than 18 different proteins are known to form amyloid fibrils, each thought to consist of short β-strands in antiparallel β-sheet conformations (*9*−*13*). Our initial modeling studies have suggested that the β-strand sequences of several amyloid proteins seem capable of forming β-helixes. The criteria we used were as follows. (a) The β-strands should form two-chain antiparallel conformations, in conformity with spectroscopic evidence (*9*−*13*). (b) All loops of random coil should coincide in successive turns of the β-helix, as established for PelC and PelE (*1*−*3*), TSP (*5*), and LpxA

S0006-2960(97)01016-7 CCC: $15.00
Published on Web 01/30/1998

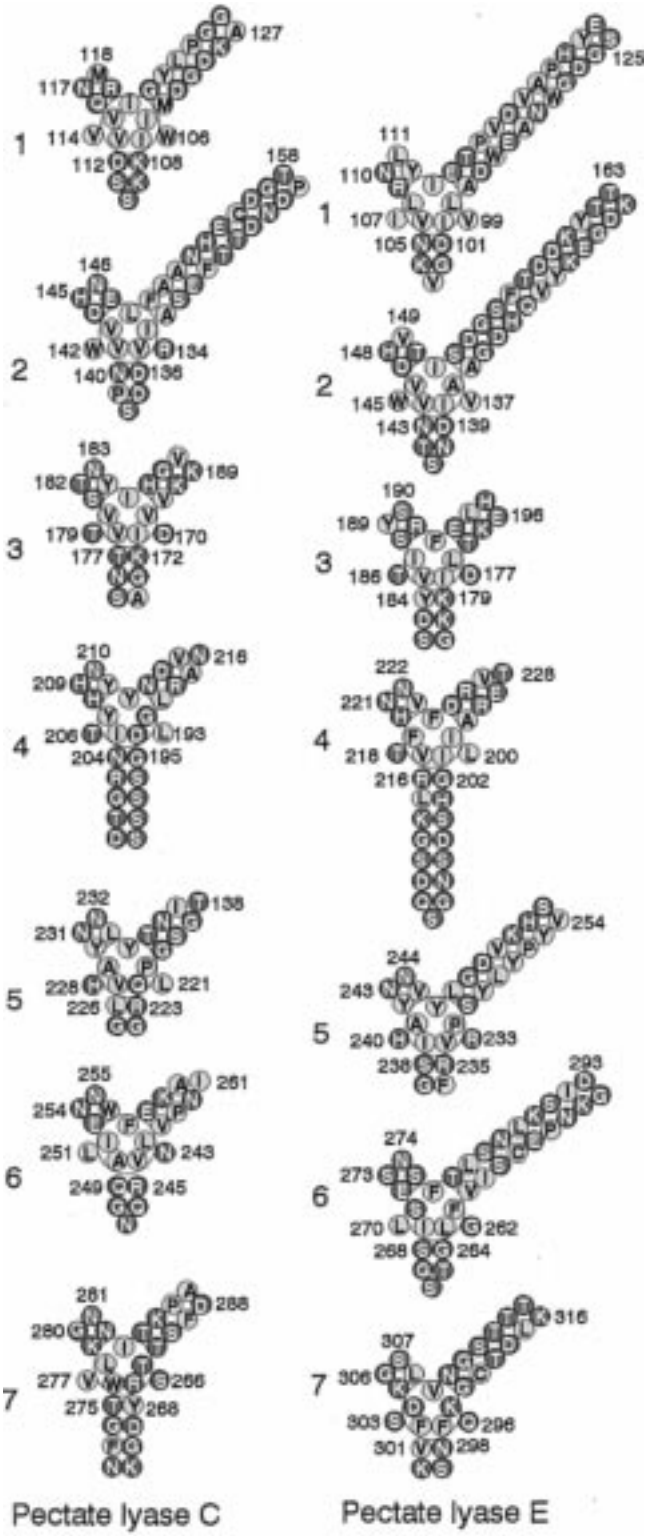

FIGURE 1: Drawings of the β-helical conformations of PelC and PelE, as determined by X-ray crystallography (*1*). The numbered structures (1−7) in each series represent successive turns of a single-chain parallel β-helix having five internal residues per turn. The small rotational offset of each turn is omitted. Hydrophobic residues are yellow, and hydrophilic residues are blue. The asparagines (N) and serines (S) that are shown in red exemplify the hydrogen bonding that can occur between residues in successive turns of the helix. Smaller-font numbers indicate sequence positions in the protein chains.

(*6*). (c) A preponderance of the residues within the lumen of the β-helix should be hydrophobic, or should be involved in intralumenal hydrogen bonding if hydrophilic. While our proposed conformations are largely conjectural, they comply with the spectroscopic, crystallographic, and microscopic data on amyloid fibrils that investigators have accumulated, and provide for the first time a scheme for accommodating the loops of random coil that are widely predicted on the basis of the primary amino acid sequences.

FIGURE 2: Axial cross section of the postulated two-chain right-handed antiparallel β-helical conformation of protofibrils of the Aβ protein of Alzheimer's plaques. Numbers 1 and 2 refer to turns of the protein chains that run in the clockwise direction, alternating with the turns 1′ and 2′ of the chains that run in the opposite direction. Smaller-font numbers indicate sequence positions in the protein chains. The degree of stagger between the antiparallel chains is that which provides the greatest number of intermolecular side chain hydrogen bonds between successive turns of the helix. Hydrophobic residues are yellow, while hydrophilic residues are blue in the clockwise chains and purple in the counterclockwise chains.

In the conformation proposed here for the Alzheimer Aβ protein (Figures 2 and 3), each of the short β-strands that are wound into the β-helix contains two internalized residues. As a result, several different degrees of stagger between the antiparallel chains could maintain the coincidence of random coil loops, and each degree of stagger would entail a different set (and a varying number) of hydrogen bonds between residues on the exterior of the helix and in loops. To determine which degree of stagger between the antiparallel chains would be most likely, each was modeled and the number of potential hydrogen bonds was counted, taking into account that each chain is contacted on both sides by the

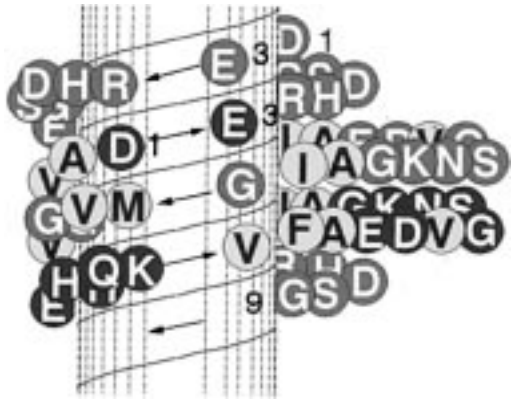

FIGURE 3: Equatorial drawing of the postulated two-chain antiparallel β-helical conformation of protofibrils of the Alzheimer Aβ protein. Arrows indicate the sequence directions of the protein chains, and the numbers indicate sequence positions in the respective chains. The color coding is like that in Figure 2.

other chain. The conformation providing the greatest number of interchain hydrogen bonds is shown in the axial view in Figure 2. We were also able to draw a lateral view of the β-helical conformation proposed for Aβ (Figure 3), which allows an assessment of the number and location of hydrophobic residues on the exterior of the helical cylinder, and in the loops of random coil, that may induce the lateral aggregation of the protofibrils.

In a similar two-chain antiparallel conformation that we propose for Rei (Figures 4 and 5), all of the constituent β-strands contain three internalized residues, and again could adopt a number of different degrees of stagger between the antiparallel chains. The conformation shown in Figure 4 was estimated to provide the greatest number of interchain hydrogen bonds. We were also able to draw lateral views (front and back) of the β-helical conformation proposed for Rei, as shown in Figure 5. This representation provides insight into the spirals of residues external to the helical cylinder that may influence the lateral aggregation of the β-helical protofibrils to form fibrils, through interactions between hydrophobic residues, or through the formation of salt bridges (*14*).

Using the same graphical conventions, expressions of a β-helical conformation were prepared for protofibrils that might be formed from the amyloid protein TTR. Figure 6 depicts a two-chain antiparallel conformation, with the degree of axial stagger of the chains that provided the largest aggregate number of interchain hydrogen bonds. The expression also revealed that the single intralumenal hydrophilic residue (Asn-124) may be capable of hydrogen bonding with its counterpart in the antiparallel chain, across the lumen of the helix.

In our formulations of the β-helical structure of amyloid protofibrils (Figures 2−6), each turn of the helix is shown to contain six hydrophobic residues in the central lumen, compared with five such residues demonstrated for the pectate lyases. This difference is imposed by the two-chain antiparallel conformation widely accepted for amyloid structures (*9*, *13*), compared with the single-chain structure of the pectate lyases. Construction of CPK models of a continuous β-helix (uninterrupted by loops of random coil) showed that the single-chain structure requires 11.3 residues per turn of the helix, while the two-chain structure requires

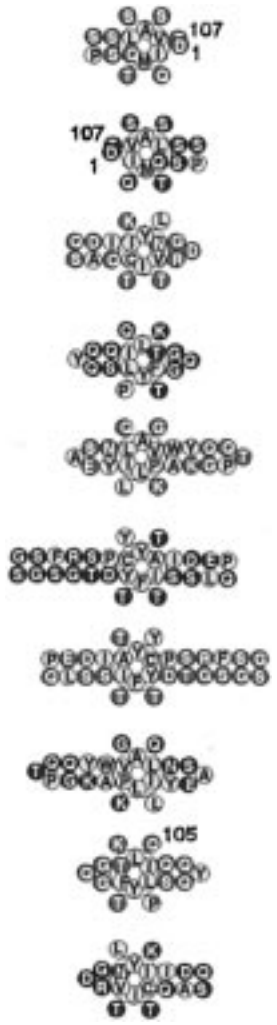

FIGURE 4: Axial cross section of the two-stranded antiparallel β-helix proposed for Rei. The degree of stagger between the antiparallel chains is that which provides the greatest number of intermolecular side chain hydrogen bonds between successive turns of the helix. The first and last residues in each sequence are numbered, and residues are color coded as in Figure 2.

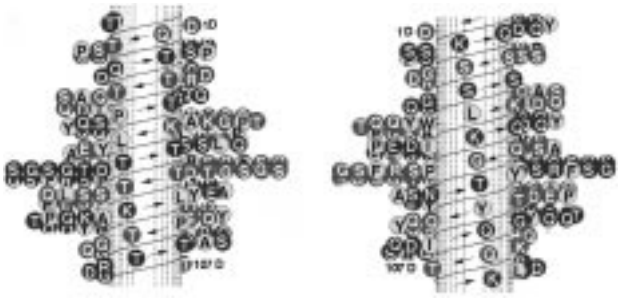

FIGURE 5: Lateral representation of the two-stranded antiparallel β-helix proposed for Rei. As determined from construction of CPK atomic models, the external amino acid side chains belonging to the β-strands form left-handed spirals on the exterior of the helix cylinder, each forming an angle of 13° with a plane passing through the axis of the cylinder. The tilt of the β-strands relative to a tangent normal to the helix axis was calculated to be 11°, on the basis of the 1.6 nm helix diameter and the 0.96 nm axial rise per turn of each chain. The color coding is like that in Figure 2.

13.3 residues per turn, in either the parallel or the antiparallel orientation (*15*). The average size of the hydrophobic residues assigned to the helix interior also affects the potential number of residues per turn in such a way that a continuous

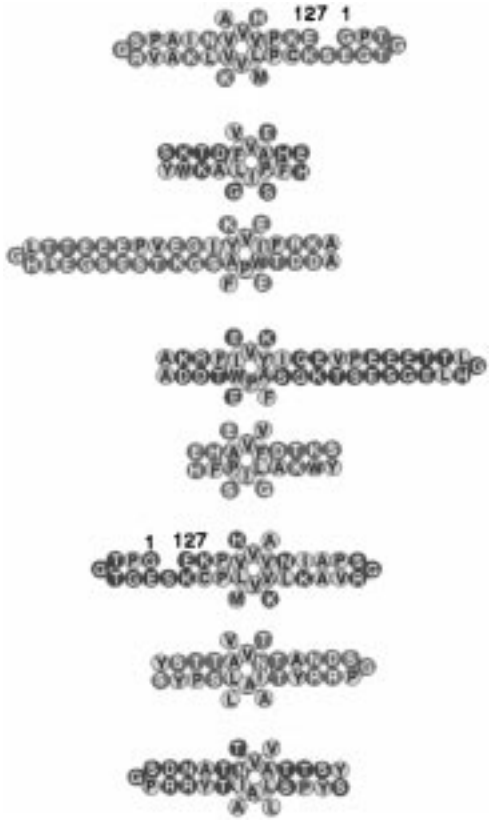

FIGURE 6: Axial cross section of TTR as a two-stranded antiparallel β-helix. The degree of axial stagger between the two antiparallel chains is that which provided the greatest number of side chain hydrogen bonds. The residues are color coded as in Figure 2, and the first and last residues in each chain are numbered.

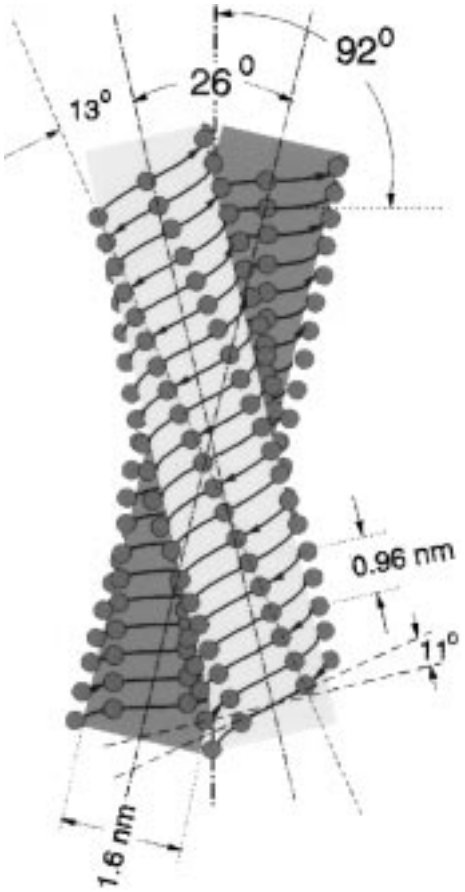

FIGURE 7: Representation of two β-helical protofibrils crossing at an angle of 26°, as required for the fit between the spirals of external residues. The imposed crossing angle ensures that the β-strands in the line of contact between any two helixes will be almost at right angles with the common axis of the helix pair.

β-helix having only alanine residues in the hydrophobic positions can be constructed with 9.3 residues per turn (not shown).

Amyloid Fibril Formation

As indicated by the construction of space-filling CPK models (*15*−*17*), and by the dimensions of protofibrils formed by synthetic peptides (*18*), the protofibrils that could be formed by the amyloid proteins would have diameters of 2 nm, in keeping with the smallest amyloid subunits observed in recent studies (*7*, *8*). Amyloid fibril formation may result only when a particular conformation favors the antiparallel condensation of protein chains, in a staggered arrangement that promotes axial propagation of the conformation, analogous to the mechanism proposed for assembly of intermediate filaments (*15*−*18*). However, the chance adoption of complementary conformations by two protein chains, simultaneously and in proper juxtaposition, must be vanishingly small. As a result, amyloid-type associations should be improbable but, once formed, may serve as a template for self-replication, using available copies of the protein. This limitation on self-replication could explain some of the characteristics of amyloid disorders, including the prion-mediated diseases.

Patients with familial amyloidotic polyneuropathy produce amyloid fibrils that are derived from variants of TTR. Transmission electron microscopy of stained cross sections showed that these fibrils have a uniform diameter of 13 nm and are composed of a bundle of four protofilaments having a center-to-center spacing of 5−6 nm (*7*). Studies using synchrotron x-radiation (*19*) produced crystallographic data suggesting a cross-β-sheet conformation, in which the transverse β-strands were stacked edge to edge to form a ribbon. Each successive β-strand was rotated radially 15° with respect to the previous one so that the ribbon was twisted 360° after 24 strands, and each strand formed an angle of close to 90° with respect to the axis of the twisted ribbon conformation. Protofilaments were proposed in which four to six ribbons (protofibrils) were stacked before twisting, and four such protofilaments, in a bundle having a square cross section, formed a fibril 13 nm in diameter (*19*). Alternatively, the β-helical conformation that we propose as a subunit for TTR fibrils in this study can be visualized as conforming to the X-ray crystallographic and electron microscopy studies of TTR fibrils (*7*, *19*). As determined from CPK models, and illustrated in Figure 7, successive strands are offset circumferentially because of the spatial requirements of the peptide hydrogen bonds between the antiparallel turns of the helix. The circumferential offset produces left-handed helical spirals of amino acid residues on the external cylindrical surface, inclined at an angle of 13° with respect to the axis of the helix. Given the 13° angle of the spirals and the 1.6 nm diameter of the helix cylinder, each spiral would accomplish a complete turn around the cylinder in 22 nm of axial length, or approximately 23 turns of a helix having a rise per turn of 0.96 nm. This compares with the 24 β-strands per turn of the postulated twisted ribbon

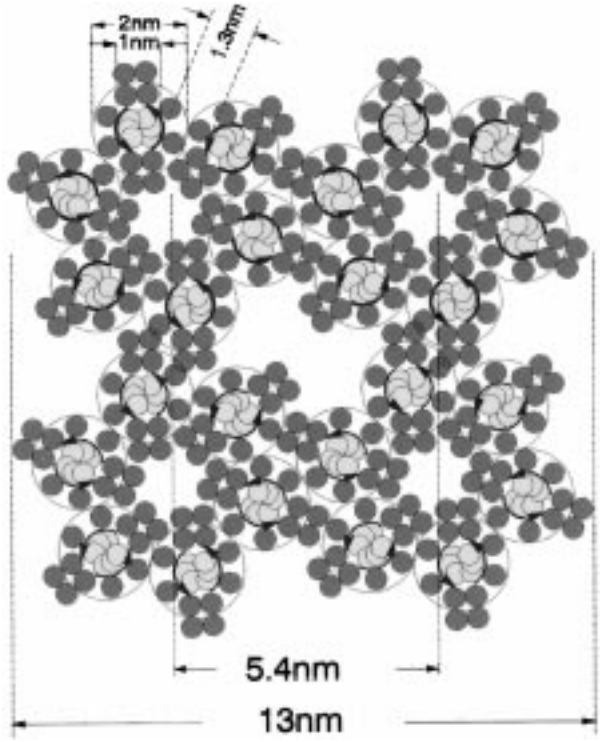

FIGURE 8: Representation of six 2 nm TTR protofibrils in each of four protofilaments forming a 13 nm fibril. The dimensions shown were estimated from CPK atomic models.

conformation (*19*). Therefore, in the conformation proposed in this study, successive β-strands in each direction would be offset about 15° circumferentially, as postulated for the rotation of successive β-strands in the twisted-ribbon model based on X-ray data (*19*).

In the TTR protofilament model of Blake and Serpell (*19*), pairs of β-strands are 1.01 nm apart, which is the spacing they would have across the lumen of the β-helix in this postulate, as measured on CPK models. The X-ray data also indicated that each pair of β-strands is separated from the next pair by a space of 1.26 nm, which approximates the spacing between β-helical protofibrils when assembled into protofilaments, as illustrated in Figures 7 and 8.

Two touching protofilaments must cross each other at an angle close to 26° to accommodate the packing of the spirals of residues on the exterior of the helixes. With the 0.96 nm axial rise of each chain, and the 1.6 nm diameter of the helix cylinder (without external side chains), the β-strands are calculated to form an angle of 11° with respect to a tangent normal to the helical axis. Therefore, the β-strands at the line of contact between each helix pair become almost normal to the common axis of the helix pair, as illustrated in Figure 7, consistent with crystallographic results (*19*).

Electron microscopy indicated a square array of four protofilaments in TTR fibrils (*7*). We propose that each of these four subunits consists of six to eight β-helical protofibrils, as illustrated in Figure 8. As shown, half of the loops of random coil that extend from the β-helical protofibrils could be packed into the central space of the protofibril bundles, and the remaining half of the loops arrayed on the exterior of the bundles. The resulting four-protofilament fibril would have a diameter close to the 13 nm assigned by electron microscopy (*7*), and the center-to-center distance between protofilaments would be 5.4 nm, consistent with the 5−6 nm spacing observed in electron micrographs (*7*). The β-helical model is therefore consistent with existing experimental evidence for the structure of several amyloid proteins, and also explains why all amyloid fibrils appear to be round, not ribbon-like or slab-like as may be expected from a cross-β structure. The provision of a universal subunit consisting of a β-helical protofibril also helps to explain how amyloid fibrils can have relatively constant diameter regardless of the sequence length of the peptide or protein from which they are aggregated. Preliminary studies have shown that each of the synthetic peptides that represent a fragment of the Aβ protein and form fibrils can be drawn as a plausible β-helix. The widely studied terminal fragment Aβ(34−42) readily forms fibrils (*13*), despite a complete absence of ionizable residues, providing support for the idea that hydrophobic interactions may be of primary importance in the aggregation of protofibrils for forming amyloid fibrils.

REFERENCES

1. Yoder, M. D., Lietzke, S. E., and Jurnak, F. (1993) *Structure 15*, 241−251.
2. Yoder, M. D., Keen, N. T., and Jurnak, F. (1993) *Science 260*, 1503−1506.
3. Yoder, M. D., and Jurnak, F. (1995) *FASEB J. 9*, 335−342.
4. Sieber, V., Jurnak, F., and Moe, G. R. (1995) *Proteins: Struct., Funct., Genet. 23*, 32−37.
5. Steinbacher, S., Seckler, R., Miller, S., Steipe, B., Huber, R., and Reinemer, P. (1994) *Science 265*, 383−386.
6. Raetz, C. R. H., and Roderick, S. L. (1995) *Science 270*, 997−1000.
7. Serpell, L. C., Sunde, M., Fraser, P. E., Luther, P. K., Morris, E. P., Sangren, O., Lundgren, E., and Blake, C. C. F. (1995) *J. Mol. Biol. 254*, 113−118.
8. Stine, W. B., Jr., Snyder, S. W., Ladror, U. S., Wade, W. S., Miller, M. F., Perun, T. J., Holzman, T. F., and Krafft, G. A. (1996) *J. Protein Chem. 15*, 193−202.
9. Sipe, J. D. (1992) *Annu. Rev. Biochem. 61*, 947−975.
10. Lai, Z., Colon, W., and Kelly, J. W. (1996) *Biochemistry 35*, 6470−6482.
11. Lansbury, P. T., Jr. (1992) *Biochemistry 31*, 6865−6870.
12. Fraser, P. E., McLachlan, D. R., Surewicz, W. K., Mizzen, C. A., Snow, A. D., Nguyen, J. T., and Kirschner, D. A. (1994) *J. Mol. Biol. 244*, 64−73.
13. Lansbury, P. T., Jr., Costa, P. R., Griffiths, J. M., Simon, E. J., Auger, M., Haverson, K. J., Kocisko, D. A., Hendsch, Z. S., Ashburn, T. T., Spenser, R. G. S., Tidor, B., and Griffin, R. G. (1995) *Nat. Struct. Biol. 2*, 990−998.
14. Stevens, F. J., Myatt, E. A., Chang, C.-H., Westholm, F. A., Eulitz, M., Weiss, D. T., Murphy, C., Solomon, A., and Schiffer, M. (1995) *Biochemistry 34*, 10697−10702.
15. Downing, D. T. (1995) *Proteins: Struct., Funct., Genet. 23*, 204−217.
16. Downing, D. T. (1996) *Proteins: Struct., Funct., Genet. 25*, 215−224.
17. Downing, D. T. (1996) *Proteins: Struct., Funct., Genet. 26*, 472−478.
18. Lazo, N. D., and Downing, D. T. (1997) *Biochem. Biophys. Res. Commun. 235*, 675−679.
19. Blake, C., and Serpell, L. (1996) *Structure 4*, 989−998.

BI971016D